Method for Optimal Actuator and Sensor Placement for Large Flexible Structures

K. B. Lim*
NASA Langley Research Center, Hampton, Virginia 23665

A method of finding the optimal sensor and actuator locations for the control of flexible structures is presented. The method is based on the orthogonal projection of structural modes into the intersection subspace of the controllable and observable subspaces corresponding to an actuator/sensor pair. The controllability and observability grammians are then used to weight the projections to reflect the degrees of controllability and observability. This method produces a three-dimensional design space wherein sets of optimal actuators and sensors may be selected. A novel parameter is introduced that is potentially useful for studying the problem of the number of actuators and sensors, in addition to their optimal locations.

Introduction

SUPPOSE a specific number of actuators and sensors is given and they are placed at specific locations on a flexible structure such that the effectiveness of the chosen actuator and sensor locations could be analyzed. If it turns out that the a priori chosen number and locations for the actuators and sensors are not sufficiently effective, the question naturally arises as to how the locations could be changed to improve the system. Furthermore, it is possible that the a priori number of actuators and/or sensors used is insufficient or redundant. Thus, there is clearly a need for a computationally feasible technique that is capable of determining an optimal set of locations and the minimal number of actuators and sensors.

In general, there will be many more candidate locations (perhaps an order of magnitude more) than the number of actuators and sensors actually available. If the number of actuators and sensors is known a priori, all possible combinations could be evaluated, and in principle, the global optimum could then be found. Unfortunately, the number of possible combinations increases factorially, and therefore an exhaustive search for a global optimal is usually computationally infeasible, while nonlinear programming based techniques typically produce local minimums.

In the past, various definitions of the degree of controllability and observability have been used in guiding the search for optimal actuator and sensor locations. Among these, the degree of controllability defined by scalar measures of recovery regions appears useful for the purpose of actuator and sensor placement.[1-3] A second approach[4] uses the projection magnitudes of eigenvectors into the input and output matrices to define gross measures of modal controllability and observability. However, only little attention is given to the development of a systematic search strategy for actually solving for an optimal set of actuators and sensors, and most attention has been directed toward defining what constitutes most suitable actuator and sensor locations.

In this paper, the problem of defining and obtaining the optimal actuator and sensor locations is addressed. A method that is based on the controllability and observability of an actuator/sensor pair is introduced. An outline of the present paper follows. First, the model of actuator and sensor locations for a linear, second-order dynamical system is presented. The basic assumption is that we are given a set of significant modes whose control is desired via feedback. In the next section, controllable, observable, and their intersection subspaces are presented, which forms the basis of the method presented in the sequel. The following section presents the main results of this paper. A cost function that is based on the weighted projection of structural modes into the intersection subspace of the controllable and observable subspaces is introduced, and a simple interpretation in terms of balanced coordinates is given. A novel method for selecting optimal sensor and actuator locations based on the preceding cost function is outlined. The weighted projections of the structural modes can be viewed as a scalar field in three-dimensional design space wherein a designer can easily select a set of actuators and sensors based on his or her own criteria without resorting to elaborate nonlinear programming strategies. The method also allows for the comparison of many actuator and sensor candidate locations since the computational effort depends only on the product of the number of actuator and sensor location candidates rather than combinatorially based search strategies whose computational effort is in the order of factorials. In the next section, the method of finding optimal locations is applied to an existing laboratory structure to demonstrate the algorithm. Finally, a few concluding remarks are given.

Actuator/Sensor Location Model

Consider the second order system

$$M\ddot{\xi}(t) + Q\dot{\xi}(t) + K\xi(t) = Eu(t) \tag{1}$$

with the translational/rotational displacement and/or velocity and/or acceleration measurements

$$y_d = F_d\xi(t); \qquad y_v = F_v\dot{\xi}(t); \qquad y_a = F_a\ddot{\xi}(t) \tag{2}$$

In the preceding equations, ξ denotes a huge finite element displacement vector (say 4000 degrees of freedom), and E is a matrix whose columns are formed from columns of identity matrix. The nonzero element for each column corresponds to the physical locations of all actuators. Each element of u denotes a physical actuator whose DOF location is defined by the location of the nonzero entry in the corresponding column in E.

For a large set of possible actuator locations (e.g., n_{act} = 300), the dimension of matrix E is 4000 × 300. F_d, F_v, and F_a are matrices of zeros and ones whose rows represent the physical locations of all displacement, velocity, and acceleration

Received July 7, 1990; presented as Paper 90-3466 at the AIAA Guidance, Navigation, and Control Conference, Portland, OR, Aug. 20-22, 1990; revision received Dec. 17, 1990; accepted for publication Dec. 21, 1990.

*Research Engineer, Spacecraft Controls Branch, Guidance and Control Division, Mail Stop 230. Member AIAA.

sensors. Similarly the sensor DOF locations are defined by the location of the nonzero entry in the corresponding rows of F_d, F_v, and F_a. For a large set of possible sensor locations for each kind (say 200), the dimensions of matrices F_d, F_v, and F_a are 200×4000 (thus $n_{\text{scn}} = 200 + 200 + 200$).

In modal form, the preceding equations can be written as

$$\ddot{\eta}(t) + \text{diag}(2\zeta\omega)\dot{\eta}(t) + \text{diag}(\omega^2)\eta(t) = \Psi^T E u(t) \tag{3}$$

$$y \triangleq \begin{Bmatrix} y_d \\ y_v \\ y_a \end{Bmatrix} = \begin{bmatrix} F_d\Psi & 0 \\ 0 & F_v\Psi \\ -F_a\Psi\ \text{diag}(\omega^2) & -F_a\Psi\ \text{diag}(2\zeta\omega) \end{bmatrix} \begin{Bmatrix} \eta(t) \\ \dot{\eta}(t) \end{Bmatrix}$$

$$+ \begin{bmatrix} 0 \\ 0 \\ F_a\Psi\Psi^T E \end{bmatrix} u(t) \tag{4}$$

where

$$\xi(t) = \Psi\eta(t) \tag{5}$$

Ψ denotes the structural mode shape vector corresponding to all n_m "significant" modes that are assumed to be known (for example, $n_m = 20$ modes and so the dimension of matrix Ψ is 4000×20). The significant modes are defined to be a subset of structural modes that are determined to be important in terms of their degree of participation in a dynamic environment, through an analysis independent of the sensors and actuators. As an example, a set of significant modes could be deduced from a combination of 1) modes that significantly influence a line-of-sight motion[5] and 2) modes that are in the bandwidth of a known disturbance.

By defining the modal state vector

$$x(t) \triangleq \begin{Bmatrix} \eta(t) \\ \dot{\eta}(t) \end{Bmatrix} \tag{6}$$

the preceding reduced system is written in the state space form

$$\dot{x}(t) = Ax(t) + Bu(t) \tag{7a}$$

$$y(t) = Cx(t) + Du(t) \tag{7b}$$

where

$$A \triangleq \begin{bmatrix} 0 & I \\ -\text{diag}(\omega^2) & -\text{diag}(2\zeta\omega) \end{bmatrix}; \qquad B \triangleq \begin{bmatrix} 0 \\ \Psi^T E \end{bmatrix} \tag{8a}$$

$$C \triangleq \begin{bmatrix} F_d\Psi & 0 \\ 0 & F_v\Psi \\ -F_a\Psi\ \text{diag}(\omega^2) & -F_a\Psi\ \text{diag}(2\zeta\omega) \end{bmatrix}$$

$$D \triangleq \begin{bmatrix} 0 \\ 0 \\ F_a\Psi\Psi^T E \end{bmatrix} \tag{8b}$$

whose eigenvalue/eigenvector equations are written as

$$A\phi_k = \lambda_k\phi_k; \qquad \|\phi_k\| = 1; \qquad k = 1, \ldots, 2n_m \tag{9}$$

The basic assumption made is that a set of n_m significant modes is known through an a priori analysis. The problem then amounts to selecting the most suitable sets of actuators and sensors for these significant modes. For the sake of discussion, a set of actuator and sensor locations is deemed most suitable if it is capable of simultaneously controlling and observing all significant modes to a high degree.

Controllable, Observable, and Intersection Subspaces

For the system given by Eq. (7), the general state transition solution is

$$x(t_1) = e^{A(t_1 - t_0)}x_0 + \int_{t_0}^{t_1} e^{A(t_1 - \tau)}Bu(\tau)\, d\tau \tag{10}$$

and, for zero initial conditions, the modal states reachable by the input $u(\tau)$, $\tau \in [t_0, t_1]$ are spanned by the range space of the controllability grammian matrix[6]

$$W^c(t_0, t_1) = \int_{t_0}^{t_1} e^{A(t_1 - \tau)}BB^T e^{A^T(t_1 - \tau)}\, d\tau \tag{11}$$

Assuming that the reduced order system is asymptotically stable (true for all vibrating flexible structures), its equilibrium solution

$$\lim_{t_1 \to \infty} W^c(t_0, t_1) \triangleq W^c_\infty = \int_0^\infty e^{A\tau}BB^T e^{A^T\tau}\, d\tau \tag{12}$$

can be computed from the Lyapunov equation

$$AW^c_\infty + W^c_\infty A^T = -BB^T \tag{13}$$

Hence, for the ith actuator, $u_i(\tau)$, $\tau \in [t_0, \infty]$, the states that can be reached are given by the range space of the ith steady state controllability grammian matrix, which is written as the eigen decomposition

$$W^c_{\infty_i} = [U_i^c \quad U_i^{c\perp}] \begin{bmatrix} \Sigma_i^c & \\ & 0 \end{bmatrix} \begin{bmatrix} U_i^{cT} \\ U_i^{c\perp T} \end{bmatrix} \tag{14}$$

where $W^c_{\infty_i}$ satisfies

$$AW^c_{\infty_i} + W^c_{\infty_i}A^T = -B_iB_i^T \tag{15}$$

$$\Sigma_i^c = \text{diag}(\sigma_1, \ldots, \sigma_{q_i^c}); \qquad \sigma_1 \geq \sigma_2 \geq \cdots \sigma_{q_i^c} > 0 \tag{16}$$

The scalar q_i^c denotes the dimension of the controllable subspace for the ith actuator location and B_i denotes the ith column of matrix B. In practice, some engineering judgment is necessary in order to define the threshold of controllability, and hence the dimension of the subspace, since the singular values typically vary gradually, down to machine epsilon (for example see Tables 1a and 1b). The columns of the U_i^c matrix form an orthogonal basis for the range space of $W^c_{\infty_i}$, and the singular values indicate the degree of importance of the corresponding column subspace in $W^c_{\infty_i}$.

Similarly, for the jth output, $y_j(\tau)$, $\tau \in [t_0, t_1]$, the states that can be observed lie in the range space of the observability grammian matrix given by

$$W_j^o(t_0, t_1) = \int_{t_0}^{t_1} e^{A^T(t_1 - \tau)}C_j^T C_j e^{A(t_1 - \tau)}\, d\tau \tag{17}$$

Its equilibrium solution takes the form

$$\lim_{t_1 \to \infty} W_j^o(t_0, t_1) \triangleq W^o_{\infty j} = \int_0^\infty e^{A^T\tau}C_j^T C_j e^{A\tau}\, d\tau \tag{18}$$

where $W^o_{\infty_j}$ satisfies

$$A^T W^o_{\infty_j} + W^o_{\infty_j}A = -C_j^T C_j \tag{19}$$

C_j denotes the jth row of matrix C. For the jth sensor, $y_j(\tau)$, $\tau \in [t_0, \infty]$, the subspace of states that can be observed is given by the range space of the jth steady state observability grammian matrix, which is written as the eigen decomposition

$$W^o_{\infty_j} = [U_j^o \quad U_j^{o\perp}] \begin{bmatrix} \Sigma_j^o & \\ & 0 \end{bmatrix} \begin{bmatrix} U_j^{oT} \\ U_j^{o\perp T} \end{bmatrix} \tag{20}$$

Table 1a Normalized singular values of controllability grammian matrix for each input 1,2,7

Input no.		
1	2	7
0.1000E + 01	0.1000E + 01	0.1000E + 01
0.9853E + 00	0.3448E + 00	0.5239E + 00
0.5903E + 00	0.8094E − 01	0.7136E − 01
0.5790E + 00	0.5907E − 01	0.6948E − 01
0.1056E + 00	0.4803E − 01	0.3624E − 01
0.4277E − 01	0.3667E − 01	0.2110E − 01
0.3317E − 01	0.2565E − 01	0.1366E − 01
0.2942E − 01	0.1494E − 01	0.3513E − 02
0.7134E − 02	0.3631E − 02	0.2983E − 02
0.1507E − 02	0.2486E − 02	0.2886E − 02
0.9347E − 03	0.1518E − 02	0.2459E − 02
0.2992E − 03	0.1008E − 02	0.7540E − 03
0.2051E − 03	0.7576E − 03	0.6321E − 03
0.1553E − 03	0.5515E − 03	0.6313E − 03
0.1373E − 03	0.2146E − 03	0.6086E − 03
0.1231E − 03	0.1863E − 03	0.5001E − 03
0.1154E − 03	0.1734E − 03	0.4521E − 03
0.1077E − 03	0.9249E − 04	0.2185E − 03
0.1013E − 03	0.6353E − 04	0.1715E − 03
0.6001E − 04	0.4819E − 04	0.5505E − 04
0.4424E − 04	0.3229E − 04	0.3365E − 04
0.2884E − 04	0.2781E − 04	0.1698E − 04
0.2512E − 04	0.1285E − 04	0.1054E − 04
0.1431E − 04	0.1264E − 04	0.6370E − 05
0.1898E − 05	0.9339E − 05	0.4990E − 05
0.1126E − 05	0.6623E − 05	0.4227E − 05
0.8987E − 06	0.5328E − 05	0.3293E − 05
0.5787E − 06	0.3217E − 05	0.1340E − 05
0.3702E − 06	0.3130E − 05	0.1207E − 05
0.3584E − 06	0.1470E − 05	0.3766E − 06
0.2356E − 06	0.9569E − 06	0.2760E − 06
0.1415E − 06	0.8318E − 06	0.2189E − 06
0.1228E − 06	0.7272E − 06	0.2036E − 06
0.8782E − 07	0.4899E − 06	0.1099E − 06
0.4218E − 07	0.4298E − 06	0.8297E − 07
0.2932E − 07	0.1845E − 06	0.5139E − 07
0.2827E − 07	0.1108E − 06	0.4414E − 07
0.1924E − 07	0.8101E − 07	0.3036E − 07
0.1438E − 07	0.7853E − 07	0.2031E − 07
0.1170E − 07	0.4906E − 07	0.7447E − 08
0.1007E − 07	0.2849E − 07	0.4374E − 08
0.1499E − 09	0.3385E − 08	0.7188E − 10

Table 1b Normalized singular values of observability grammian matrix for each output 4,5,6

Output no.		
4	5	6
0.1000E + 01	0.1000E + 01	0.1000E + 01
0.8677E + 00	0.1462E + 00	0.3542E + 00
0.7133E − 01	0.1084E + 00	0.2370E + 00
0.6892E − 01	0.4975E − 01	0.1730E + 00
0.5588E − 01	0.2165E − 01	0.3292E − 01
0.2899E − 01	0.1530E − 01	0.1586E − 01
0.1636E − 01	0.1378E − 01	0.1327E − 01
0.1132E − 01	0.6742E − 02	0.1104E − 01
0.6029E − 02	0.4106E − 02	0.8340E − 02
0.3072E − 02	0.3585E − 02	0.3370E − 02
0.5332E − 03	0.1220E − 02	0.1921E − 02
0.4803E − 03	0.9280E − 03	0.1752E − 02
0.4669E − 03	0.4043E − 03	0.1681E − 02
0.3516E − 02	0.1238E − 03	0.4964E − 03
0.2098E − 03	0.1182E − 03	0.2942E − 03
0.1820E − 03	0.6845E − 04	0.2911E − 03
0.1566E − 03	0.3724E − 04	0.2877E − 03
0.4224E − 04	0.2944E − 04	0.2526E − 03
0.3340E − 04	0.1822E − 04	0.1692E − 03
0.2733E − 04	0.1096E − 04	0.1410E − 03
0.2636E − 04	0.8060E − 05	0.9399E − 04
0.2605E − 04	0.7616E − 05	0.5520E − 04
0.1394E − 04	0.6682E − 05	0.2950E − 04
0.1290E − 04	0.5956E − 05	0.2902E − 04
0.1036E − 04	0.5929E − 05	0.2637E − 04
0.8530E − 05	0.4014E − 05	0.1557E − 04
0.8427E − 05	0.3120E − 05	0.1179E − 04
0.7920E − 05	0.1840E − 05	0.7420E − 05
0.1828E − 05	0.1794E − 05	0.6447E − 05
0.9672E − 06	0.1709E − 05	0.5087E − 05
0.7293E − 06	0.7223E − 06	0.4467E − 05
0.7219E − 06	0.3722E − 06	0.1998E − 05
0.5327E − 06	0.3101E − 06	0.1234E − 05
0.4922E − 07	0.9708E − 07	0.4898E − 06
0.4723E − 08	0.8749E − 07	0.9626E − 07
0.2878E − 08	0.2098E − 07	0.7635E − 07
0.1679E − 09	0.5441E − 08	0.3664E − 07
0.1119E − 09	0.3196E − 08	0.2504E − 07
0.9862E − 10	0.1803E − 09	0.3534E − 08
0.6606E − 10	0.7882E − 11	0.1224E − 08
0.1521E − 12	0.4656E − 11	0.3393E − 11
0.7963E − 13	0.3114E − 11	0.1776E − 11

where

$$\Sigma_j^o = \text{diag}(\sigma_1, \ldots, \sigma_{q_j^o}); \qquad \sigma_1 \geq \sigma_2 \geq \cdots \sigma_{q_j^o} > 0 \quad (21)$$

The scalar q_j^o denotes the dimension of the observable subspace for the jth sensor location. The columns of the U_j^o matrix form an orthogonal basis for the range space of $W_{\infty_j}^o$, and the singular values indicate the degree of importance of the corresponding column subspace in $W_{\infty_j}^o$.

The subspace of states that can be both observed and controlled by the ith actuator and the jth sensor is given by the intersection subspace

$$S_{ij} \triangleq R(U_i^c) \cap R(U_j^o) \quad (22)$$

where $R(\,)$ denotes the range space. Note that any state vector that is unobservable and/or uncontrollable does not lie in the aforementioned intersection subspace. For the ith actuator and jth sensor pair, the intersection subspace dimension and a corresponding orthogonal basis can be computed via singular value decomposition as follows[7]: let

$$D_{ij} \triangleq U_j^{oT} U_i^c \quad (23)$$

Then, the dimension of the ijth intersection subspace d_{ij} is given by the number of singular values of the matrix D_{ij} that takes the value of unity, so that

$$D_{ij} = [Y_{ij} \quad Y_{ij}^{\perp}] \begin{bmatrix} \Sigma_{ij} & \\ & \Sigma_{ij}' \end{bmatrix} \begin{bmatrix} Z_{ij}^T \\ Z_{ij}^{\perp T} \end{bmatrix} \quad (24)$$

where

$$\Sigma_{ij} = \text{diag}(\cos\theta_1, \ldots, \cos\theta_{d_{ij}}) = I_{d_{ij}}$$
$$\Sigma_{ij}' = \text{diag}(\cos\theta_{d_{ij}+1}, \ldots, \cos\theta_{\hat{q}_{ij}}); \qquad \cos\theta_l < 1 \quad (25)$$
$$l = d_{ij} + 1, \ldots, \hat{q}_{ij}$$
$$\hat{q}_{ij} \triangleq \min(q_i^c, q_j^o)$$

and $I_{d_{ij}}$ denotes an identity matrix of dimension d_{ij}. An orthogonal basis for the ijth intersection subspace S_{ij} is given by

$$S_{ij} = U_j^o Y_{ij} \quad (26)$$

In practice, the diagonal elements of Σ_{ij} will not be exactly 1 due to limitations in the accuracy of the numerical computations, and the cosine of the principal angles, $\theta_1, \ldots, \theta_{d_{ij}}$, which are measures of the distance between two subspaces, may not be exactly unity. Therefore, a value $(1 - \epsilon)$ must be used to define an intersection threshold.

Optimal Actuator and Sensor Locations

In the preceding section, the dimensions of the intersection subspaces could be computed for all candidate locations to arrive at d_{ij} for $i = 1, \ldots, n_{\text{act}}$, $j = 1, \ldots, n_{\text{sen}}$. Note that the dimension of the intersection subspace is bounded by

$$0 \leq d_{ij} \leq \hat{q}_{ij} \quad (27)$$

with $q_i^c \leq n_m$ and $q_j^o \leq n_m$. It can be observed that the larger the value of d_{ij}, the more suitable is the ijth actuator/sensor pair location; i.e., the subspace of states that can be simultaneously observed and controlled is larger. Hence, one may decide to choose actuator and sensor location pairs corresponding to the largest value of d_{ij} in a descending order. A potential pitfall of the above strategy is that the dimension of the intersection subspace may not necessarily indicate the number (or degree) of modes contained in the intersection subspace. Hence, the dimension d_{ij} may not be a reliable indicator of the number (or degree) of simultaneously controllable and observable modes. Therefore, we next investigate the breakdown of the intersection subspace in terms of the modal components by using orthogonal projections.

For the ijth intersection subspace, the orthogonal projection of kth mode, ϕ_k, onto S_{ij} is

$$\phi_k^{ij} = S_{ij} S_{ij}^T \phi_k \tag{28}$$

A geometrical interpretation of the projection in an intersection subspace is shown in Fig. 1. It should be emphasized that the approach introduced herein uses a *single* projection into an intersection subspace as compared with a strategy based on independent projections into controllability and observability subspaces. Note that two independent projections will result in two different projection components, and hence combined indices based on the weighted sum (or products) of the projection magnitudes may lead to physically meaningless indices.

Although the projected eigenvector state ϕ_k^{ij} is both controllable and observable, its degree of controllability and observability is yet undetermined. To reflect this degree, the controllability and observability grammians are used in a combined index such that

$$\alpha_k^{ij} \triangleq \left(\phi_k^{ijT} W_{\infty_i}^c \phi_k^{ij}\right)\left(\phi_k^{ijT} W_{\infty_j}^o \phi_k^{ij}\right) \tag{29}$$

Geometrically speaking, observe from Fig. 1 that the preceding combined index takes the largest possible value if 1) the eigenvector ϕ is completely (or almost completely) contained in the intersection subspace S_{ij} and 2) the projected eigenvector ϕ^{ij} (if the eigenvector is not completely contained in S_{ij}) is parallel (or nearly parallel) to both the directions of maximum controllability $u_{i_1}^c$ and maximum observability $u_{j_1}^o$. The controllability and observability grammians are used to weight the orthogonal projections of all n_m significant modes into all combinations of actuator and sensor candidate locations, so that we obtain

$$\alpha_k^{ij}; \quad k = 1, \ldots, n_m; \quad i = 1, \ldots, n_{\text{act}}$$
$$j = 1, \ldots, n_{\text{sen}} \tag{30}$$

The problem reduces to choosing for each mode k a pair of locations that gives a maximum value of α_k^{ij}. Considering a total of n_m modes, this strategy provides a set of $\bar{n}_a$ actuator locations and $\bar{n}_s$ sensor locations that are globally optimal where

$$\bar{n}_a \leq \min(n_m, n_{\text{act}}) \tag{31a}$$

$$\bar{n}_s \leq \min(n_m, n_{\text{sen}}) \tag{31b}$$

Note that as many as n_m actuators and sensors may be necessary. A brief summary of the computational procedure follows:

Step 1: For $i = 1, \ldots, n_{\text{act}}$
  Step 1.1: Compute $W_{\infty_i}^c$ From Eq. (15)
  Step 1.2: Compute U_i^c from Eq. (14)
  Step 1.3: Store U_i^c, $W_{\infty_i}^c$
  Next i
Step 2: For $j = 1, \ldots, n_{\text{sen}}$
  Step 2.1: Compute $W_{\infty_j}^o$ from Eq. (19)
  Step 2.2: Compute U_j^o from Eq. (20)
  Step 2.3: For $i = 1, \ldots, n_{\text{act}}$
    Step 2.3.1: Compute D_{ij} from Eq. (23)
    Step 2.3.2: Compute Y_{ij} and d_{ij} from Eq. (24)
    Step 2.3.3: Compute α_k^{ij}; $k = 1, \ldots, n_m$ from Eq. (29)
    Next i
  Next j
Step 3: Find $\max_{ij}(\alpha_k^{ij})$; $k = 1, \ldots, n_m$

In the search for the maximum projection pair (i,j) for mode k in step 3, there may be several pairs of (i,j) that give the maximum or near-maximum values for the eigenvector projection magnitudes. For mode k, let Γ^k denote the set of pairs that are maximum or near-maximum and define a residual projection R_k^{ij} for each pair $(i,j) \in \Gamma^k$,

$$R_k^{ij} \triangleq \sum_{l=1, l \neq k}^{n_m} \alpha_l^{ij} \tag{32}$$

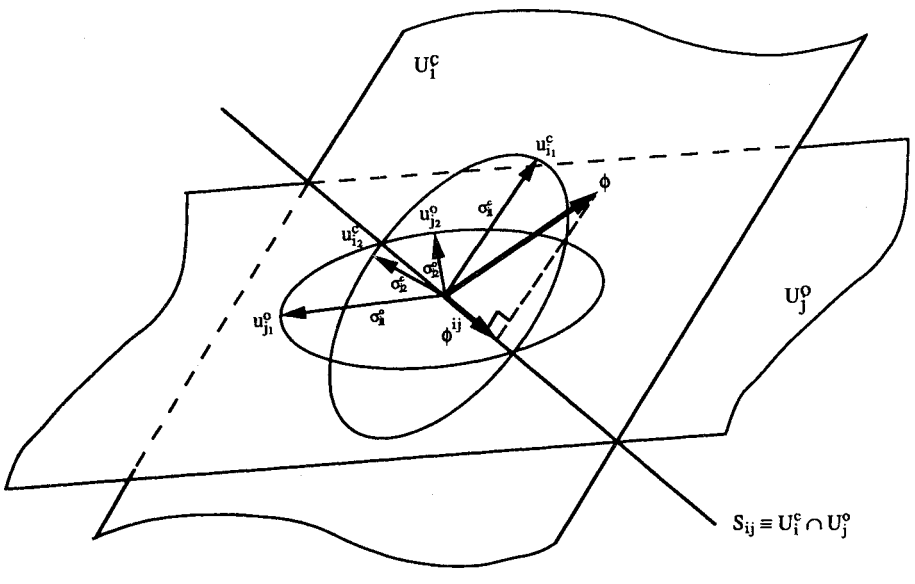

Fig. 1 Weighted projection on intersection subspace.

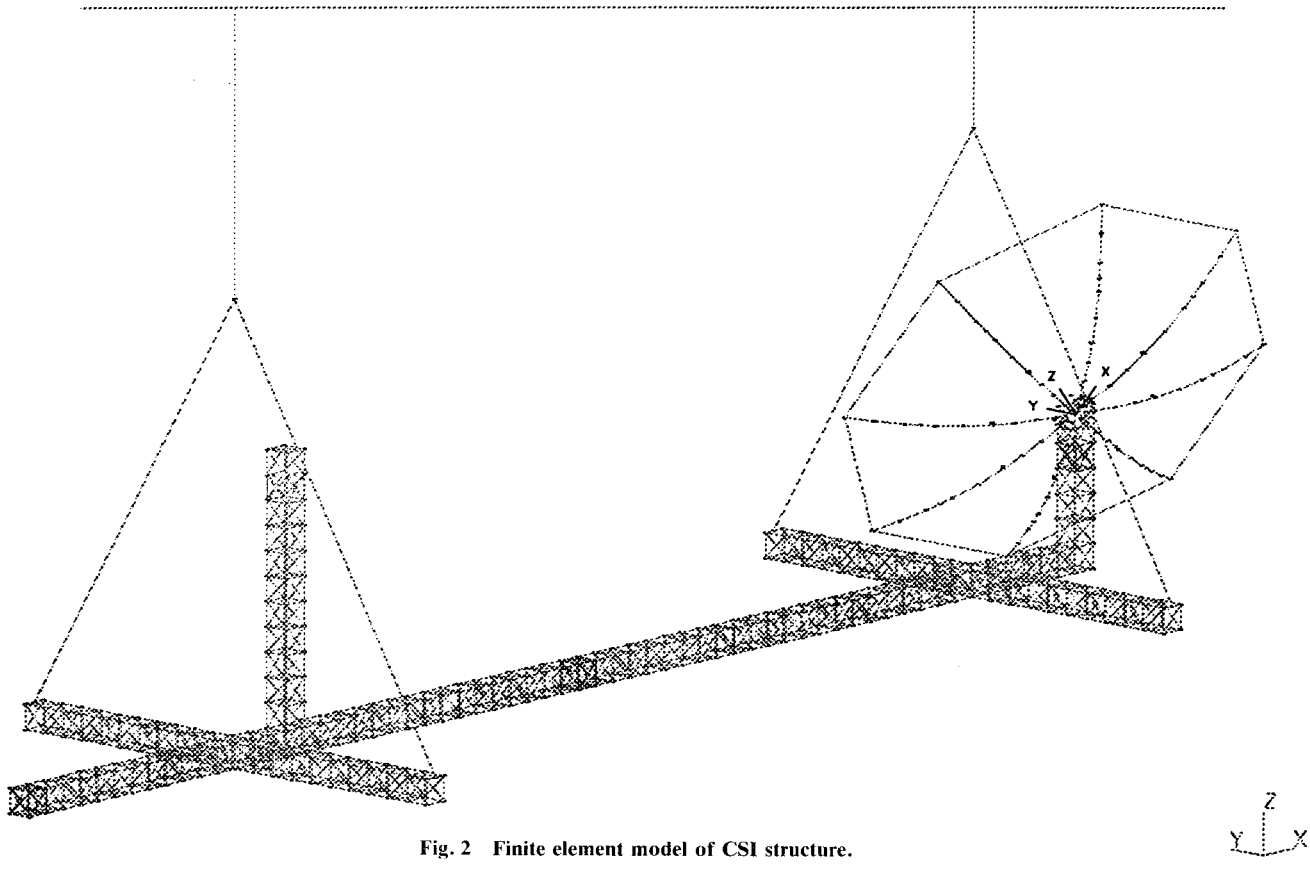

Fig. 2 Finite element model of CSI structure.

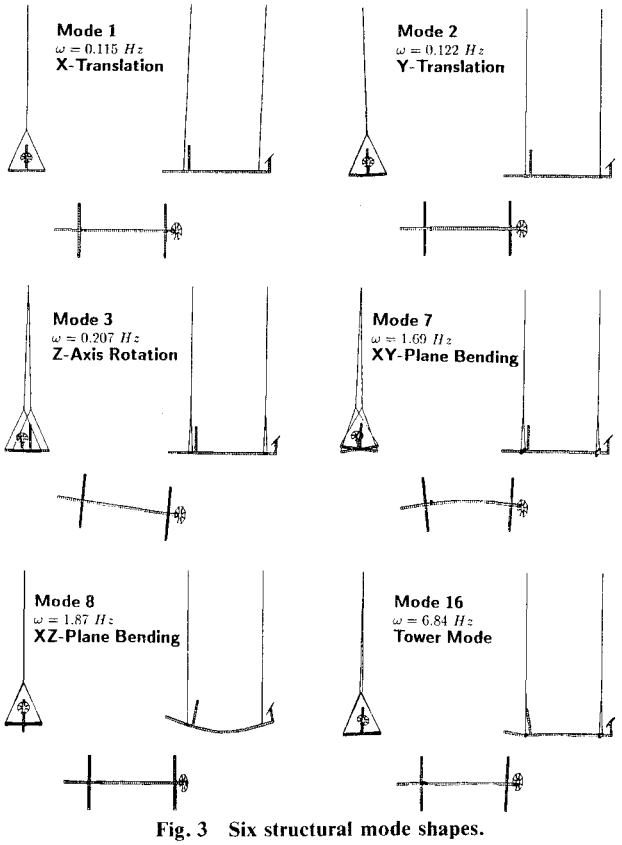

Fig. 3 Six structural mode shapes.

For this multiple or near-multiple case, a strategy based on selecting the (i,j) pair within the set Γ^k having the largest residual projection is proposed; i.e.,

$$\max_{\Gamma^k} R_k^{ij} \tag{33}$$

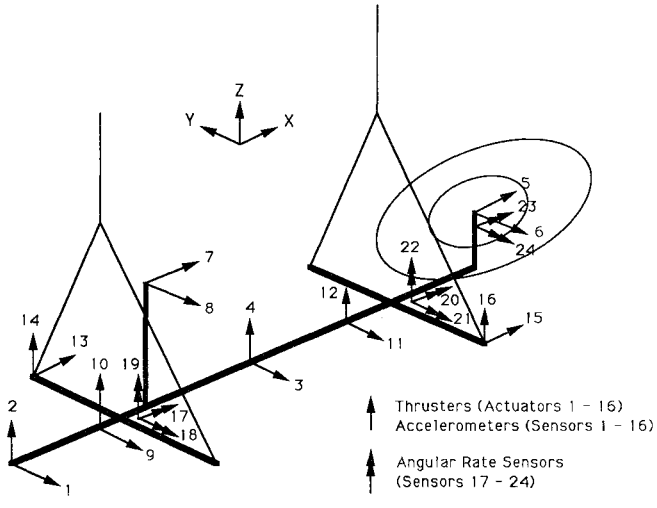

Fig. 4 Actuator and sensor locations.

The rationale for the preceding strategy is that the selection of the pair having a larger residual projection corresponds to more versatile pairs. This criterion obviously encourages a net smaller set of actuator and sensor pairs. Note that the search for the optimal location is based on the three-dimensional design space defined by α_k^{ij}, $i = 1, \ldots, n_{\text{act}}$, $j = 1, \ldots, n_{\text{sen}}$, $k = 1, \ldots, n_m$.

The combined index given in Eq. (29) simplifies considerably in a particularly significant set of coordinates. It is well known[8] that for a completely observable and controllable system, a particular similarity transformation can be used to transform to balanced coordinates for each (i,j) pair. In balanced coordinates, the grammians are equal and diagonal; i.e.,

$$\tilde{W}_{\infty_i}^c = \tilde{W}_{\infty_j}^o = \tilde{\Sigma}_{ij} = \text{diag}(\tilde{\sigma}_1, \ldots, \tilde{\sigma}_{n_m}) \tag{34}$$

where $\tilde{\sigma}_1 \geq \tilde{\sigma}_2 \geq \tilde{\sigma}_{n_m} > 0$, and the tilde denotes balanced coordinates. The corresponding controllable/observable orthogonal basis simplifies to [cf. Eqs. (23) and (26)]

$$\tilde{D}_{ij} = \tilde{S}_{ij} = I_{n_m \times n_m} \tag{35}$$

and the orthogonal projection of the kth mode in $\tilde{S}_{ij}$ is [cf. Eqs. (28)]

$$\tilde{\phi}_k^{ij} = P_{ij}^{-1} \phi_k \tag{36}$$

where P_{ij} denotes the similarity transformation matrix corresponding to the (i,j)th balanced coordinates. Finally, the combined index of Eq. (29) simplifies to

$$\alpha_k^{ij} \triangleq (\tilde{\phi}_k^{ij\prime} \tilde{\Sigma}_{ij} \tilde{\phi}_k^{ij})(\tilde{\phi}_k^{ij\prime} \tilde{\Sigma}_{ij} \tilde{\phi}_k^{ij}) = \|\tilde{\phi}_k^{ij}\|_{\tilde{\Sigma}_{ij}}^2 \tag{37}$$

The above combined index is equivalent to a norm of the kth eigenvector in (i,j)th balanced coordinates weighted by the second-order modes,[8] which captures the input-output properties of the (i,j)th system. Physically, the balanced coordinate transformation decomposes the eigenvector in terms of equally controllable and observable states and then weights the balanced states according to their degrees of controllability and observability. Note that the combined index in Eq. (29) is not restricted to minimal systems.

Application to Controls-Structure Interaction Laboratory Structure

To illustrate the application of the algorithm, let us consider the problem of placing actuators and sensors on the controls-structure interaction (CSI) testbed structure at NASA Langley Research Center[5] (see Fig. 2). The control design model consists of 21 significant structural modes whose maximal controllability and observability are desired for the purpose of active vibration suppression. Figure 3 shows a subset of six mode shapes. Among the modes shown, the first three are pendulum modes, the next two are modes 7 and 8 corresponding to the first truss beam bending mode in the XY and XZ planes, respectively, and the last mode shown is a tower mode. The remaining modes (not shown) include very complex mode shapes due to the coupling of multiaxis bending and twisting of substructures such as the antenna dish, main bus, tower beam, and suspension cables. Sixteen candidate locations for thrust actuators are considered along with 16 accelerometers and 8 angular rate sensors as shown in Fig. 4. It should be mentioned that the first 16 actuators and sensors are not perfectly collocated as they appear in Fig. 4 and are in fact offset by one half of a bay, which is of dimension $10 \times 10 \times 10$ in.

Tables 1a and 1b show the normalized singular values of the controllability and observability grammians (in descending order) corresponding to a typical single actuator and sensor respectively. The numerical values indicate the *degree* of controllability and observability. While it is true that the above grammian matrices are not exactly singular, hence strictly speaking fully controllable and observable, their degrees of controllability and observability vary widely from 8 (actuator 2) to 13 (sensor 4) orders of magnitude. Physically, this means that for actuator 2 a hundred million times more control effort may be required to produce the same control effect as the most controllable mode; i.e., the mode is practically uncontrollable. Notice also from the tables that the degree of controllability and observability varies gradually in most cases. Figures 5a and 5b show the typical singular values of the controllability and observability grammians (in descending order) corresponding to two sets of eight actuators and eight sensors. Case 1 is the result of a heuristically based actuator and sensor location analysis while case 2 is the result of applying the optimal actuator and sensor location algorithm. The actuator and sensor locations for both figures are

Case 1:

Inputs [1 2 3 4 5 6 7 8]

Outputs [1 2 3 4 5 6 7 8]

Case 2:

Inputs [1 2 4 7 8 13 15 16]

Outputs [1 2 4 7 8 13 15 16]

Notice that case 2 generally produced larger singular values, which indicates improved controllability and observability.

To give an idea of computational requirements to solve the preceding problem, consider the problem of placing exactly 8

Table 2 Dimension d_{ij} of intersection subspaces[a]

Sensor no.	Actuator no.															
	1	2	3	4	5	6	7	8	9	10	11	12	13	14	15	16
1	34	34	33	35	25	32	32	34	31	32	35	33	34	35	34	35
2	35	35	30	36	28	33	35	35	32	33	32	34	35	36	35	36
3	33	33	32	34	24	31	31	33	30	31	34	32	33	34	33	34
4	33	33	28	34	27	31	33	33	30	31	30	32	33	34	33	34
5	35	35	30	36	28	33	35	33	30	33	32	34	35	36	35	36
6	37	37	34	38	28	35	35	37	34	35	36	36	37	38	37	38
7	35	35	30	36	28	33	35	33	30	33	32	34	35	36	35	36
8	34	34	33	35	25	32	32	34	31	32	35	33	34	35	34	35
9	33	33	32	34	24	31	31	33	30	31	34	32	33	34	33	34
10	35	35	30	36	28	33	35	35	32	33	32	34	35	36	35	36
11	34	34	33	35	25	32	32	34	31	32	35	33	34	35	34	35
12	35	35	30	36	28	33	35	35	32	33	32	34	35	36	35	36
13	37	37	33	38	30	35	35	35	32	35	35	36	37	38	37	38
14	37	37	32	38	28	35	37	37	34	35	34	36	37	38	37	38
15	38	38	33	39	31	36	36	36	33	36	35	37	38	39	38	39
16	39	39	34	40	30	37	37	39	36	37	36	38	39	40	39	40
17	39	39	34	40	30	37	37	39	36	37	36	38	39	40	39	40
18	38	38	33	39	31	36	37	36	33	36	35	37	38	39	38	39
19	37	37	34	38	28	35	35	37	34	35	36	36	37	38	37	38
20	38	38	33	39	29	36	36	38	35	36	35	37	38	39	38	39
21	40	40	35	41	32	38	38	38	35	38	37	39	40	41	40	41
22	37	37	34	38	28	35	35	37	34	35	36	36	37	38	37	38
23	39	39	34	40	30	37	37	39	36	37	36	38	39	40	39	40
24	34	34	29	35	28	32	32	34	31	32	31	33	34	35	34	35

[a] $\sigma_{\min}/\sigma_{\max} = 10^{-4}$

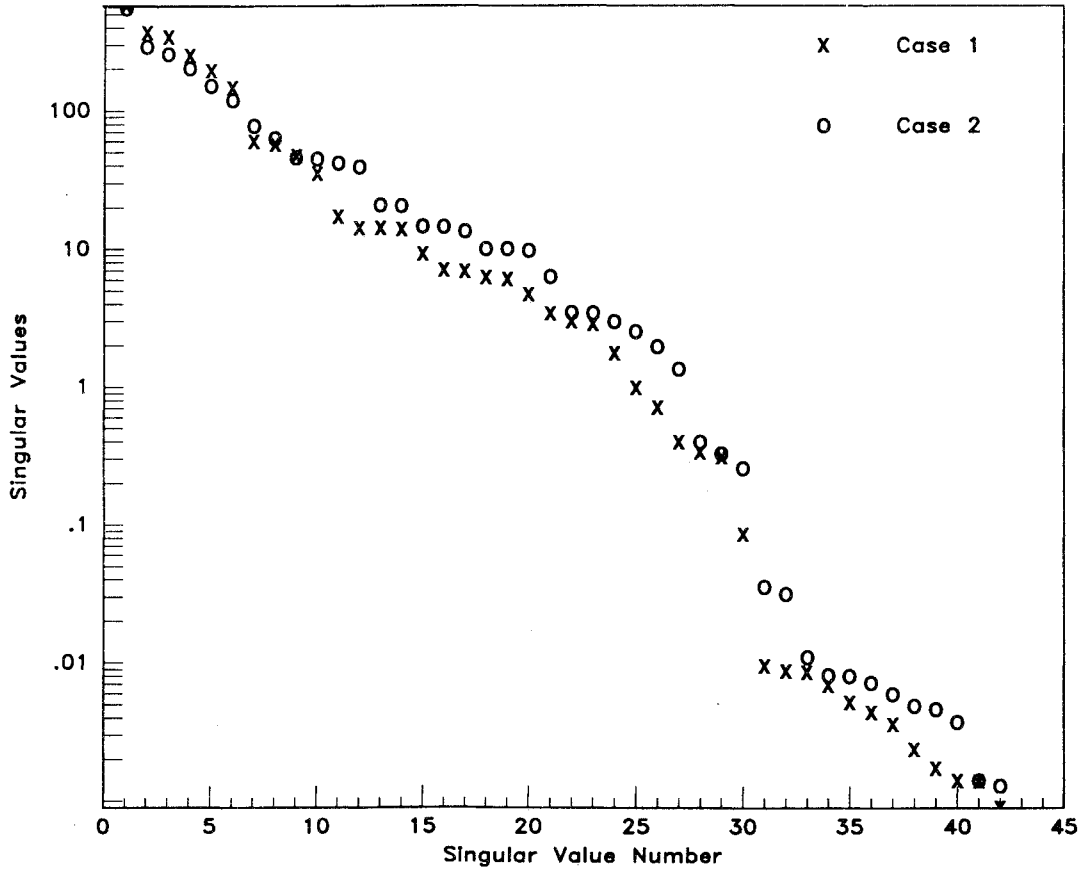

Fig. 5a Singular values of controllability grammian.

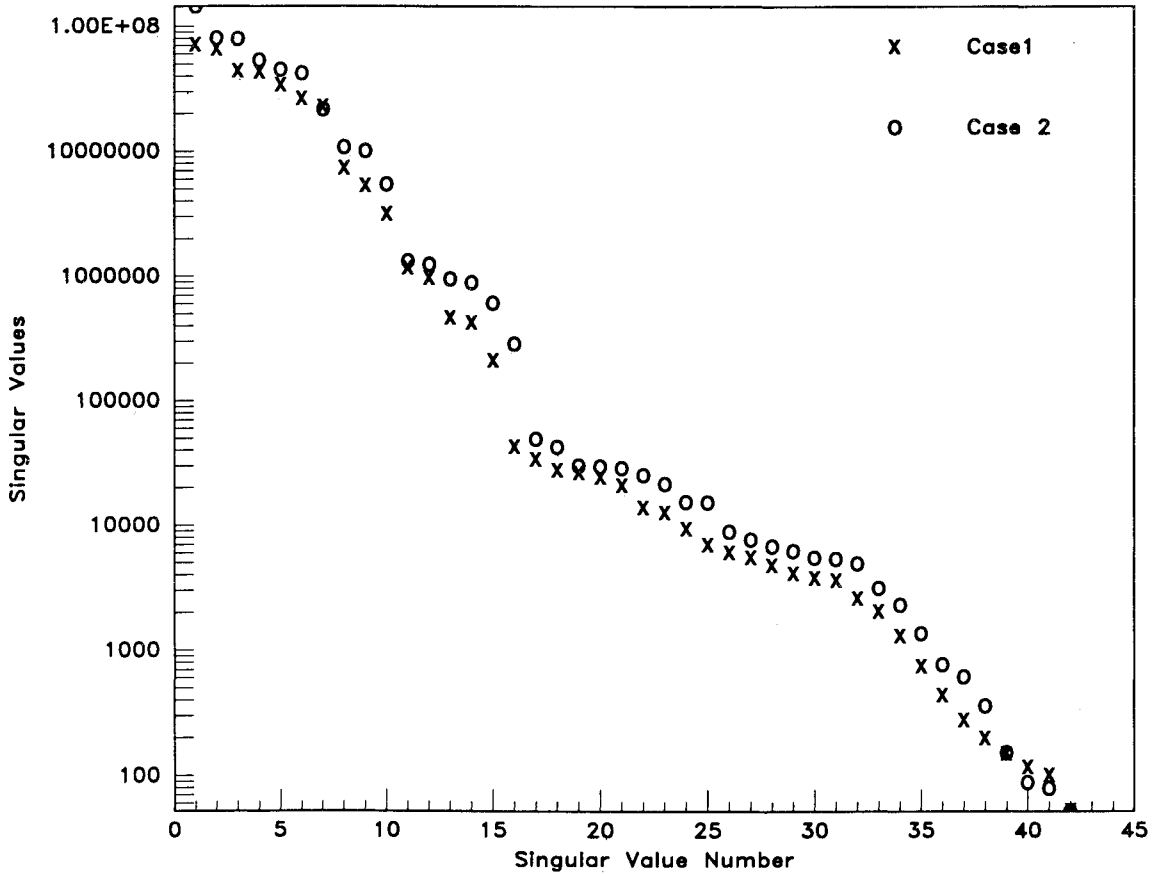

Fig. 5b Singular values of observability grammian.

Table 3 Optimal locations for sensors and actuators[a]

Mode no.	Actuator no.	Sensor no.	α_k^{ij}	No. of maximums	Residual
1	7	7	0.5311E + 04	16	0.1029E + 07
2	11	11	0.6903E + 04	2	0.2211E + 05
3	1	1	0.3521E + 05	1	0.3309E + 06
4	16	16	0.2203E + 05	1	0.3611E + 06
5	2	2	0.1140E + 06	1	0.1970E + 06
6	8	8	0.3678E + 06	1	0.6271E + 06
7	1	1	0.4821E + 05	1	0.3179E + 06
8	2	2	0.1033E + 06	1	0.2077E + 06
9	16	16	0.1902E + 06	1	0.1929E + 06
10	16	16	0.5776E + 05	1	0.3253E + 06
11	2	2	0.5094E + 04	1	0.3059E + 06
12	15	15	0.1152E + 06	1	0.2947E + 06
13	2	2	0.3769E + 05	1	0.2733E + 06
14	8	8	0.5833E + 06	1	0.4117E + 06
15	15	15	0.1798E + 06	1	0.2301E + 06
16	7	7	0.7095E + 06	1	0.3252E + 06
17	8	8	0.8682E + 04	1	0.9863E + 06
18	7	7	0.2064E + 06	1	0.8283E + 06
19	4	5	0.9602E + 04	1	0.1014E + 05
20	13	13	0.1741E + 06	1	0.4299E + 06
21	13	13	0.3610E + 06	1	0.2430E + 06

[a] $\hat{\alpha}_k = 0.01$, $\sigma_{min}/\sigma_{max} = 10^{-4}$

Table 4 Versatility vs effectiveness[a]

	Actuator/sensor no., $\hat{\alpha}_k$						
Mode no.	0.999	0.990	0.900	0.500	0.100	0.010	10^{-5}
1	7	7	7	7	7	7	7
2	8	8	8	1	11	11	11
3	8	8	1	1	1	1	1
4	14	14	16	16	16	16	16
5	7	14	14	2	2	2	2
6	8	8	8	8	8	8	8
7	8	8	8	16	1	1	1
8	7	7	7	7/2	2	2	2
9	8	8	14	16	16	16	16
10	14	16	16	16	16	16	16
11	7	7	2	2	2	2	2
12	8	8	13	15	15	15	15
13	7	7	7/2	2	2	2	2
14	14	14	14	8	8	8	8
15	8	8	7	15	15	15	15
16	13	16	7	7	7	7	7
17	7	8	8	8	8	8	8
18	7	7	7	7	7	7	7
19	7	7	7	4	4	4/5	4/5
20	8	8	13	13	13	13	13
21	8	13	13	13	13	13	13
Total no. of actuators	4	5	7	8	9	9	9
Sensors	4	5	7	8	9	9	9

[a] $\sigma_{min}/\sigma_{max} = 10^{-4}$

sensors on 24 candidate locations. To compute the grammian matrices corresponding to all possible combinations, we require

$$C(24,8) = \frac{24!}{(24-8)!8!} = 735{,}471$$

solutions of a 42-order symmetric Lyapunov equation. Since a single symmetric Lyapunov equation requires[9] approximately $5n^3 = 5 \times 42^3 = 370{,}440$ multiplications, a 100 MFlop supercomputer would need about 45 min of CPU time. If the problem size doubles to 48 candidate sensor locations, then

$$C(48,8) = \frac{48!}{(48-8)!8!} = 377{,}348{,}994$$

combinations are possible, which translates to about 16 days of CPU time. On the other hand, the approach proposed in this paper requires $48 \times 16 = 768$ solutions of symmetric Lyapunov equations, which requires only about 2.8 s CPU time. The fact is that the computational effort necessary in an exhaustive search for a global optimum may be overwhelming, even for a modestly sized problem, because the computational effort grows *factorially* whereas the effort required by the proposed approach grows *linearly* with the size of the problem.

Table 2 shows the dimension of intersection subspaces due to 24 sensor and 16 actuator candidates. It can be seen that out of a possible intersection space dimension of 42, the dimensions range from 24 to 41. A threshold singular value of the grammian matrices used to define controllability and observability subspaces for Table 2 is 10^{-4} with a maximum singular value of 1. More tolerable threshold singular values will produce larger dimensioned intersection subspaces. Note that the sensor/actuator pairs corresponding to the larger dimensions

can be selected by inspection. Although larger row sums (or column sums) generally indicate more effective sensors and actuators, as noted earlier, this dimension in state space may not indicate the number and degree of modes contained in the intersection subspace and hence may not be a reliable indicator.

Table 3 lists the optimal locations for sensors and actuators. A total of nine actuators and sensors is recommended. From the mode shapes shown in Fig. 3, it can be seen that the actuator/sensor pair selected for each mode is intuitively correct. For example, for mode 3, which is a yawing pendulum motion, the actuator 1 and sensor 1 pair is selected. Notice that actuator 1 has the largest moment arm to generate yawing motion as compared with actuators 3, 6, 8, 9, 11, 13, or 15. It is interesting to note from Table 3 that the optimal sensor and actuator location pair for each mode (except mode 19) is a collocated configuration. This indicates the dual nature of the controllability and observability problems. Obviously this result is possible only if the candidate locations allowed for the sensors and actuators are similar. For sensors, only accelerometers are selected over angular rate sensors. This is not unexpected because acceleration signals are larger than angular rate signals for this particular vibrating structure.

Table 4 shows the effect of varying the threshold used for defining near-maximums so that the set Γ^k can be identified. Notice that for the case with only four actuators and sensors, the actuators and sensors, consisting of 7, 8, and 14, form an orthogonal set that appears intuitively correct for the control and detection of multiaxis motion (21 significant structural modes). In this study, the threshold $\hat{\alpha}_k$ is defined such that a pair $(i,j) \in \Gamma^k$ if

$$(\alpha_k - \alpha_k^{ij})/\alpha_k \leq \hat{\alpha}_k \tag{38}$$

where

$$\alpha_k \triangleq \max_{ij} \alpha_k^{ij} \tag{39}$$

More tolerable threshold values (larger $\hat{\alpha}_k$) produce a larger number of near-maximums, and this encourages the selection of more versatile actuator and sensor pairs. This results in a net smaller set of actuators and sensors. The preceding parameter may therefore be used for studying the problem of optimal locations as well as the problem of selecting the number of actuators and sensors.

Concluding Remarks

A novel method of selecting actuator and sensor locations that are optimal, based on the combined degree of controllability and observability of each structural mode, has been developed. The selection is based on the *effectiveness* (controllability and observability of a particular mode) and *versatility* (controllability and observability of all modes) of pairs of actuators and sensors. The method introduced herein is not based on nonlinear programming nor does it require an a priori specification of the number of actuators and sensors. A new parameter that may physically be interpreted as an indicator of the degree of *versatility/effectiveness* is introduced for studying the problem of the selection of the number of actuators and sensors as well as the problem of optimal locations. The method has been demonstrated on the model of an existing laboratory structure.

In applying this method to a design problem it is recommended that the design begin with a small set of candidate locations that are probably heuristically based. If application of this method produces a subset of these actuator and sensor locations that allows sufficient controllability and observability of all significant modes, then the design problem is solved. Otherwise, additional locations can be added to the candidate set, and the new computations associated only with the added locations can be made to determine and evaluate a new set of optimal locations.

It should be noted that typically a set of closed loop performance (vibration suppression, command tracking, disturbance rejection, stability robustness, etc.) is the ultimate objective of the optimal locations of actuators and sensors. Consequently, the precise benefit of a location strategy based on any open loop analysis may vary depending on the specific control objective and the control law under consideration. However, the physical implications of a measure of the degree of controllability and observability are an appropriate indicator of the suitability of a plant to any type of feedback control.

References

[1]Viswanathan, C. N., Longman, R. W., and Likins, P. W., "A Degree of Controllability Definition: Fundamental Concepts and Application to Modal Systems," *Journal of Guidance, Control, and Dynamics,* Vol. 7, No. 2, 1984, pp. 220-230.

[2]Viswanathan, C. N., Longman, R. W., and Likins, P. W., "A Definition of the Degree of Controllability—A Criterion for Actuator Placement," *Proceedings of the Second VPI&SU/AIAA Symposium on Dynamics and Control of Large Flexible Spacecraft,* edited by L. Meirovitch, Virginia Polytechnic Inst. and State Univ., Blacksburg, VA, June 1979.

[3]Longman, R. W., Sirlin, S. W., Li, T., and Sevaston, G., "The Fundamental Structure of Degree of Controllability and Degree of Observability," *AIAA/AAS Astrodynamics Specialists Conference,* AAS Paper 82-1434, San Diego, CA, 1982.

[4]Hamdan, A. M. A., and Nayfeh, A. H., "Measures of Modal Controllability and Observability for First- and Second-Order Linear Systems," *Journal of Guidance, Control, and Dynamics,* Vol. 12, No. 3, 1989, pp. 421-428.

[5]Lim, K. B., and Horta, L. G., "A Line-of-Sight Performance Criterion for Controller Design of a Proposed Laboratory Model," AIAA Paper 90-1226, April 1990.

[6]Brockett, R. W., *Finite Dimensional Linear Space,* Wiley, New York, 1970.

[7]Golub, G. H., and VanLoan, C. F., *Matrix Computation,* Johns Hopkins Univ. Press, Baltimore, MD, 1985, p. 430.

[8]Moore, B. C., "Principal Component Analysis in Linear Systems: Controllability, Observability, and Model Reduction," *IEEE Transactions on Automatic Control,* Vol. AC-26, No. 1, 1981, pp. 17-32.

[9]Bartels, R. H., and Stewart, G. W., "Algorithm 432: Solution of the Matrix Equation $AX + XB = C$," *ACM,* Vol. 15, No. 9, 1972, pp. 820-826.